

Fabrication of Gold Nanoparticles by Pulsed Laser Ablation in Aqueous Media

Dongfang YANG, Seongkuk LEE, Bo CHEN and Suwas NIKUMB

*Industrial Materials Institute, National Research Council Canada
800 Collip Circle, London, Ontario, N6G 4X8, Canada
E-mail: Dongfang.yang@nrc.gc.ca*

The growth of Au nanoparticles by laser ablation processes has been systematically investigated. The morphology of Au metal nanoparticles was characterized with respect to laser wavelength, pulse duration, pulse energy, and surfactant concentrations in order to understand the nanoparticle formation process during laser ablation. Three different laser wavelengths including a nanosecond excimer laser operating at 248 nm, femto-second Ti:Sapphire laser operating at 776 nm and nanosecond diode-pumped Nd:YAG laser operating at its second harmonic wavelength of 532 nm were used for Au nanoparticles fabrication in surfactant-free and surfactant-containing aqueous solutions. Field emission SEM, XRD and UV-visible absorption spectrum were used for the characterization of Au nanoparticles. The parameters controlling the morphology of Au nanoparticles during laser ablation in surfactant-free and surfactant-containing aqueous media are discussed. It was found that particle size and size distribution of Au nanoparticles produced by nanosecond Nd:YAG and KrF excimer lasers are less affected by the laser fluence than that of femtosecond Ti:Sapphire laser.

Keywords: nanoparticle, laser ablation, gold, surfactants

1. Introduction

The Nanoparticles of noble metals are very attractive for applications in various areas such as catalysis, optics, and life environments [1]. This is due to the quantum confinement and/or interfacial effects in nanocrystallites that induce many unique properties, which are different from those of bulk materials. The growth of nanoparticles by laser ablation process, although it is widely used as conventional fabrication process, is still not fully understood due to its complexity [2-4].

In this paper, we have carried out a systematic investigation of the morphology of Au nanoparticles characterized with respect to laser wavelength, pulse duration, pulse energy, repetition rate, and other laser process parameters in order to understand the nanoparticle formation process during laser ablation. Au nanoparticles were fabricated by pulsed laser ablation of an Au foil using three different laser wavelengths with either nanosecond or femtosecond pulse duration in surfactant-free and surfactant-containing aqueous solutions. Both alkanethiols (i.e. 1-butanethiol $n\text{-C}_4\text{H}_9\text{SH}$) and ionic surfactants sodium alkyl sulfates (i.e. Sodium dodecyl sulfate $\text{C}_{12}\text{H}_{25}\text{SO}_4\text{Na}$) aqueous solutions with various concentrations were used to stabilize the Au nanoparticles once they are formed by laser ablation. Field emission SEM, X-ray diffraction (XRD) and UV-visible absorption were used for the characterization of Au nanoparticles. The parameters controlling the morphology and properties of Au nanoparticles during laser ablation in surfactant-free and surfactant-containing aqueous media are discussed.

2. Experimental Details

The experiments were carried out with a femtosecond Ti:Sapphire laser (CPA-2010, Clark MXR, $\lambda = 776$ nm and

pulse width = 150 fs), second harmonic Nd:YAG laser (YHP-40, Spectra Physics, $\lambda = 532$ nm and pulse width = 15 ns), and KrF Excimer laser (LPX-210, Lambda Physik, $\lambda = 248$ nm and pulse width = 25 ns). As shown in Figure 1, the focused beam was irradiated perpendicularly onto a piece of 25 μm thick Au metal foil (99.95% pure, from Goodfellow), which was placed and fixed at the bottom of Teflon vessel containing aqueous solution. Pure deionized water, sodium dodecyl sulfate ($\text{C}_{12}\text{H}_{25}\text{SO}_4\text{Na}$), or 1-butanethiol ($n\text{-C}_4\text{H}_9\text{SH}$) was chosen as the aqueous solutions. The concentration of sodium dodecyl sulfate and 1-butanethiol was varied in the range of $10^{-3} \sim 10^{-4}$ M.

During laser ablation experiments using Ti:Sapphire laser and second harmonic Nd:YAG laser, the vessel was placed on the x-y translation stages. The stages were linearly moved at a constant feedrate (10 mm/min for Ti:Sapphire laser and 100 mm/min for Nd:YAG laser) to form rectangular ablated region of 5×2 mm² on the target surface. A total of 6×10^6 pulses was irradiated at a fixed repetition rate (femtosecond: 1 kHz, Nd:YAG: 10 kHz), and the pulse energy was varied in the range of 1.8 ~ 12.1 J/cm² for Nd:YAG laser and 1.3 ~ 25.7 J/cm² for Ti:Sapphire laser. Meanwhile, the experiment with Excimer laser was carried out at a stationary mode, 300 pulses with the energy density of 5 J/cm² were irradiated at the repetition rate of 50 Hz.

During laser ablation in stationary liquid containing surfactant, bubbles were generated in solution or hemispheric bubbles were adhered to the surface shielded laser radiation. The incident light is also scattered by the bubbles rising upward. To avoid this, a jet of air was used to blow away the bubbles to minimize this effect. The focal plane was maintained on the surface of the target.

After gold nanoparticle suspensions were produced by the laser ablation, a few drops of the suspension were dropped on the top of a piece of single crystal (100) silicon wafer and let dried. The crystal structures of the dried Au nanoparticles fabricated at various conditions were examined by X-ray diffraction (XRD, Philips, X-Pert MRD) in the θ_0 - 2θ thin film configuration, where θ_0 was fixed at 0.5° . The dried Au nanoparticles were also investigated by Hitachi's FE-SEM S-4500 using the new super ExB filter technology. FE-SEM images were recorded at a magnification of 100,000 with a 5 kV or 15 kV beam voltage. Plasmon absorption spectrum was recorded for the Au nanoparticle suspensions in the 400-850 nm wavelength range using a fiber-optic-based spectrophotometer (Scientific Computing International, Film Tek 3000).

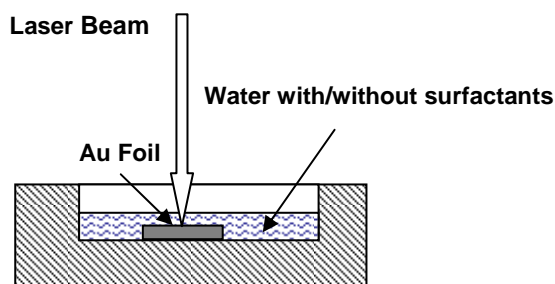


Fig. 1 Experimental set-up for laser ablation of Au nanoparticles

3. Results and Discussions

Figure 2 shows the FE-SEM micrographs of Au nanoparticles produced by the femtosecond Ti:Sapphire laser and nanosecond Nd:YAG laser ablation in 10^{-3} M $C_{12}H_{25}SO_4Na$ solutions. The laser pulse energy was increased from just above threshold of ablation (top panel) to relatively higher pulse energy (bottom panel). Left-column graphs are Au nanoparticles produced by Nd:YAG laser, while the right-column graphs are by Ti:Sapphire laser. Most of particles produced by femtosecond Ti:Sapphire at lower energy density is very small (< 20 nm). As energy density increases, large particles (> 50 nm) appear in addition to the fine particles (< 20 nm). This might be attributed to the two different ablation mechanisms at lower or higher pulse energy when femtosecond laser is used. Near the ablation threshold, Au nanoparticles are produced by the photon induced ablation mechanism. The plasma induced ablation becomes dominant with the increase of the pulse energy. However, many aspects of the phenomenon remain unclear [2,5]. Since more particles were produced as the pulse energy increases, they tended to aggregate together to form clusters. At $78 \mu J$, many big clusters which consist of many big (> 200 nm) and medium (50~100 nm) as well as small (~ 20 nm) particles appeared in addition to small particles and clusters. It seems that $C_{12}H_{25}SO_4Na$ surfactant cannot function well to separate them from aggregating together at high laser pulse energy. This may due to instant rate of evaporation by femtosecond laser pulse is so high that there is not enough time for surfactants to cover all the newly generated particles. In contrast, when nanosecond Nd:YAG laser was used for the ablation, almost none clusters appear in the suspension and the Au particles separated

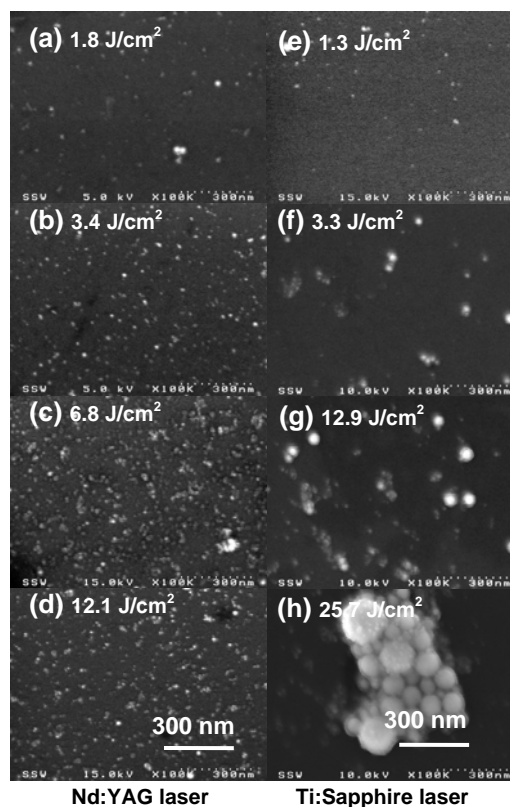


Fig.2 FE-SEM images of Au nanoparticles prepared by Ti:Sapphire laser and Nd:YAG laser ablation in 10^{-3} M $C_{12}H_{25}SO_4Na$ solution with various pulse energies).

from each other. The particle size only very slightly increased as the pulse energy increased. Particle size at low energy is less than 20 nm while at high energy more slightly larger particles (20~30 nm) appear. For both laser wavelengths, more nanoparticles were produced within the same ablation processing time when the energy density was increased as also can be seen in the Figure 2. For laser with the similar on-target fluence, the particle size of Au nanoparticles produced by femtosecond laser is much bigger than that by nanosecond laser such as shown in Figure 2b and 2f, as well as in Figure 2d and 2g. In the femtosecond laser ablation, all the Au species (atoms, ions, particles) was ablated from the target surface within such a short time that they do not have time to separate from each other before they are aggregated together to form bigger particles or clusters. In addition, less laser energy was lost to the target as thermal energy for femtosecond laser than for nanosecond laser due to shorter laser-material interaction time, which results in more Au species were ablated at each femtosecond laser pulse than at each nanosecond laser pulse. This could also contribute to bigger particles produced by femtosecond laser at higher laser energy. Figure 2 clearly indicates that nanosecond Nd:YAG laser could be better choice than femtosecond Ti:Sapphire for the fabrication of high quality Au nanoparticles (e.g., smaller particles and narrower particle size distributions) since the particle size and size distribution is less affected by the laser fluence for nanosecond laser. In order to understand the difference in the particles size distribution between two lasers, detailed information about plasma parameters is required.

It has been shown that laser ablation in liquid produces surface charged nanoparticles with a shell of dipole molecules (i.e., water) formed around them [6]. The water shell cannot prevent particle aggregation and unambiguously nanoparticles will assemble together to form large clusters in long term. Addition of various surfactants in the solution is commonly used to control and stabilize the nanoparticle suspension. Surfactants adsorb on the nanoparticle surface through either forming chemical bonds or electrostatic interaction between ionic surfactants and nanoparticles, and prevent them from aggregating together. The concentration of surfactants is believed to be one of the important parameters to control the growth and eventually the size of nanoparticles. Figure 3 shows the Au nanoparticles produced by three different laser wavelengths (e.g., femtosecond Ti:Sapphire, nanosecond Nd:YAG and nanosecond KrF excimer lasers) in water, 10^{-4} M and 10^{-3} M $C_{12}H_{25}SO_4Na$ solutions. For the nanosecond Nd:YAG and

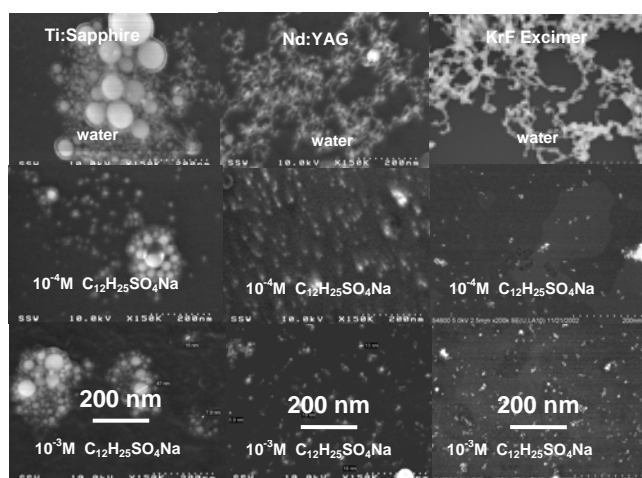


Fig.3 FE-SEM images of Au nanoparticles prepared by three different wavelength laser beams in water, 10^{-4} M and 10^{-3} M $C_{12}H_{25}SO_4Na$ solutions.

excimer lasers, laser ablation of Au foil in water produced Au nanoparticles/nanowires that aggregated together to form big network. As freshly formed Au nanoparticles are very reactive and have very high surface energy. They tend to self assemble together to reduce their surface energy. The Au nanoparticle produced by femtosecond Ti:Sapphire ablation in water, however, aggregated to form much smaller clusters that consist of spherical Au particles of large, medium and small size. Actually, the color of Au nanoparticle suspension produced by femtosecond laser in water has pink color that is very different than those suspensions produced by nanosecond laser in water which are always black. The pink color remains for long time while suspensions produced by nanosecond lasers were unstable and black particles precipitated to the bottom of the vessel from the suspensions in a few hours. This may be due to the difference in surface state/surface energy of Au nanoparticles produced by nanosecond and femto second lasers. When $C_{12}H_{25}SO_4Na$ surfactant was introduced into the water, nanosecond Nd:YAG and KrF excimer produce very fine and separated particles, while femto second Ti:Sapphire laser still produced many clusters besides the nanoparticles similar to situation in water. Another interesting observation is that in the 10^{-4} M $C_{12}H_{25}SO_4Na$ solution

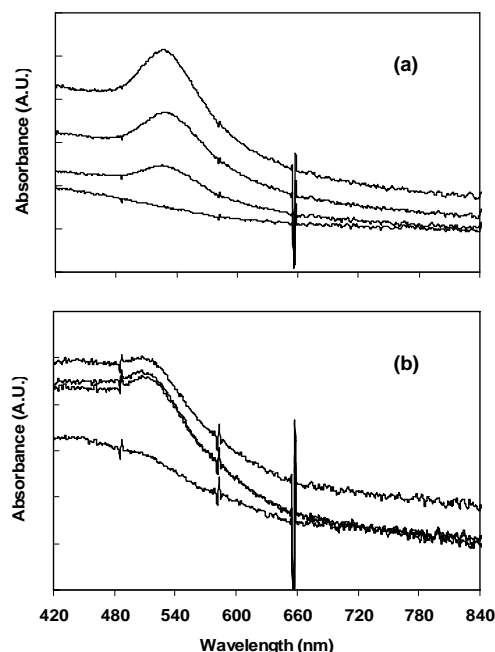


Fig. 4 Visible absorption spectra of Au nanoparticles obtained in 10^{-3} M $C_{12}H_{25}SO_4Na$ solutions under femto-second Ti:Sapphire (a) and nanosecond Nd:YAG (b) lasers ablation.

Au nanoparticles produced by nanosecond laser are the smallest with narrower particle size distributions. Most of the particles produced by nanosecond Nd:YAG and KrF excimer lasers in 10^{-4} M $C_{12}H_{25}SO_4Na$ are less than 15 nm. Slightly larger Au particles were produced in 10^{-3} M $C_{12}H_{25}SO_4Na$ by the nanosecond lasers.

UV-Visible absorption spectroscopy was also used to characterize the optical properties (i.e., color) of Au nanoparticle suspensions, since the absorption bands are related to the diameter and aspect ratio of the Au nanoparticles. Au nanoparticle suspensions show different colors when different wavelength lasers and pulse energies were used to produce them. These colors are not only absent for the bulk material, but also for the atoms. The origin of such colors and hence the strong absorption bands (resonances) in the visible region is attributed to the collective oscillation of the free conduction electrons induced by an interacting electromagnetic field. These resonances are termed surface plasmons. Figure 4 shows the visible absorption spectra of Au nanoparticles obtained in 10^{-3} M $C_{12}H_{25}SO_4Na$ solutions under femto-second Ti:Sapphire and nanosecond Nd:YAG laser ablation. The pulse energies corresponding to absorption spectra from bottom to top for Ti:Sapphire laser (figure 4a) are 4, 10, 39 and 70 μ J, while for Nd:YAG laser (figure 4b) they are 16, 31, 62 and 110 μ J, respectively. The peak in the absorption spectrum, associated with the excitation of surface plasmons, for Au nanoparticle suspension produced by Ti:Sapphire is located at 532 nm, while it is at 513 nm for that produced by the Nd:YAG laser. The peak intensity increases with the increase in the laser pulse energy indicating more Au nanoparticles were produced in the same ablation time. However, the absorption peak position does not shift much which suggests that average particle size does not vary much with pulse energy. However, this observation may

not be true for lowest pulse energy (just above ablation threshold) since the absorption peak cannot be seen clearly. It was reported that for 3-30 nm Au nanoparticles the plasmon-related peak is around 520 nm [7]. Under the experimental conditions, this peak was around 532 nm by Ti:Sapphire laser ablation and 513 nm by Nd:YAG laser ablation. This is consistent with FE-SEM observation that Ti:Sapphire produced many larger sizes nanoparticle clusters in the suspension while Nd:YAG laser produced small and separated nanoparticles.

Figure 5 shows XRD patterns of Au nanoparticles fabricated by femto-second Ti:Sapphire and nanosecond Nd:YAG lasers in pure water and in 10^{-3} M $C_{12}H_{25}SO_4Na$ solutions. The diffraction patterns consist of three main diffraction peaks at around 38.3° , 44.5° and 64.8° for Au nanoparticles produced by Ti:Sapphire laser, and 38.5° , 44.8° and 65.1° by Nd:YAG laser, respectively. The three main diffraction peaks represent the (111), (200) and (220) orientations of Au particles as they match to the XRD ref-

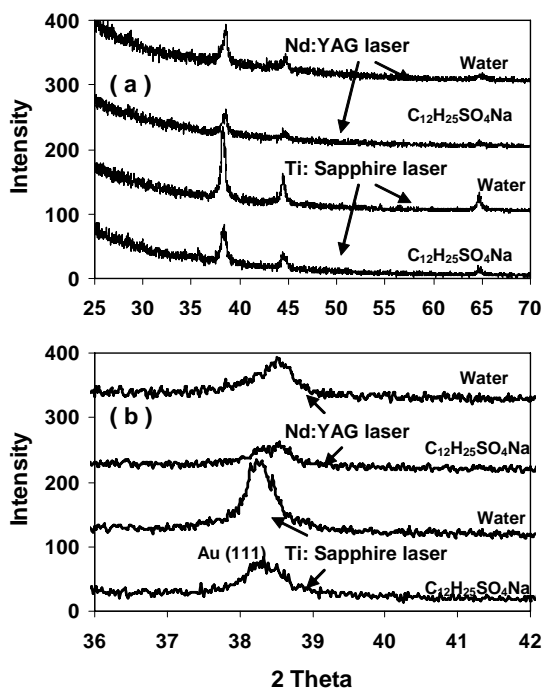


Fig.5 XRD patterns of Au nanoparticles prepared by femto-second Ti:Sapphire and nanosecond Nd:YAG lasers in pure water and 10^{-3} M $C_{12}H_{25}SO_4Na$ solutions. Figure 5b is the expansion of Au(111) peak in figure 5a.

erence JCPDS 04-0784 for bulk Au, whose 2θ angles are 38.2° , 44.4° and 64.6° respectively. The results clearly illustrate that the lattice constants of Au nanoparticles are smaller than those of bulk Au. The lattice constants of Ti:Sapphire laser ablated nanoparticles are larger than those of Nd:YAG laser ablated nanoparticles. Another interesting observation is that the existence of the surfactant $C_{12}H_{25}SO_4Na$ in the solution does not affect the lattice constants for both nanosecond and femtosecond lasers as the peak positions are almost the same for solution with or without surfactant. The pulse duration of lasers used, seems to have more important impact on the lattice constants of

nanoparticles. It is well known that the full width at half-maximum (FWHM) of XRD peak contains information about the average particle size according to the Scherrer formula. The FWHM of 38° XRD peak for Ti:Sapphire laser ablated nanoparticles in water and in 10^{-3} M $C_{12}H_{25}SO_4Na$ as shown in figure 5b are 0.43° and 0.59° 2θ , while they are 0.59° and 0.63° for Nd:YAG laser ablated nanoparticles in water and in 10^{-3} M $C_{12}H_{25}SO_4Na$ respectively. These numbers indicate that Ti:Sapphire laser produced larger average particle size Au nanoparticles (may be due to existing of clusters) than the Nd:YAG laser did, and laser ablation in the present of $C_{12}H_{25}SO_4Na$ surfactant produced smaller particles than in the presence of pure water.

Sodium dodecyl sulfate (SDS) was commonly used to control the particle growth in aqueous solutions, which enabled in reducing the mean size of Au and Ag nanoparticles down to 4-8 nm and to minimize the particle size dispersion down to 5 nm [8-11]. Mercaptan (e.g., alkanethiol) is known to adsorb strongly on the gold surface to form self-assembling monolayer which is initiated by strong chemical interactions between the sulfur and gold surface. This interaction is considered as a result of chemisorption that forced a thiorate molecule to adsorb commensurate with a gold lattice. Then, the tail-to-tail interaction of the molecules created by lateral interchain nonbonded interactions, which is strong enough to align the molecules parallel on the gold surface and create a crystalline film [12]. Therefore, alkanethiol could be a good surfactant candidate to control the Au particle growth during laser ablation. Since alkanethiols with long alkane chain almost do not dissolve in water, only short chain alkanethiols, such as n-1-butanethiol n- C_4H_9SH , can be used as aqueous surfactants. Figure 6 shows the FE-SEM images of Au nanoparticles fabricated by KrF excimer laser ablation in 10^{-3} M $C_{12}H_{25}SO_4Na$ and 10^{-3} M n- C_4H_9SH solutions, respectively. KrF laser ablation of Au foil in n- C_4H_9SH produced Au nanoparticles with particle size ranging from 5 nm to 20 nm with some of them aggregated together. Laser ablation of Au foil in $C_{12}H_{25}SO_4Na$ then produced much smaller nanoparticles. They are ranging from 2 nm up to 10 nm with less aggregation. Results from figure 6 clearly indicated that by simply using different surfactant, the particle size could be controlled. With the same molar concentration, laser ablation in ionic surfactant $C_{12}H_{25}SO_4Na$ produces smaller particles than in butanethiol. This may be due to the longer chain length of $C_{12}H_{25}SO_4Na$ than C_4H_9SH which can effectively separate nanoparticles from each other and block their aggregation.

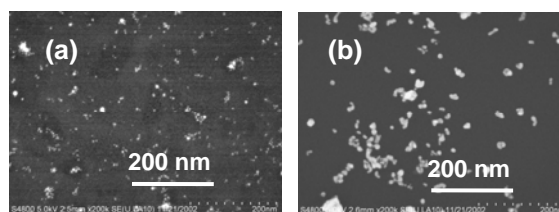


Fig. 6 FE-SEM images of Au nanoparticles fabricated by KrF excimer laser ablation in (a) 10^{-3} M $C_{12}H_{25}SO_4Na$ and (b) 10^{-3} M n- C_4H_9SH solution.

4. Conclusion

Three different wavelength lasers including a nanosecond excimer and diode pumped Nd:YAG lasers and a femtosecond Ti:Sapphire laser have been used to ablate a gold target to produce gold nanoparticles in water and surfactant containing aqueous solutions of sodium dodecyl sulfate and 1-butanethiol in order to understand the parameters that govern the growth and size of Au nanoparticles. Particle size and size distribution of gold nanoparticles produced by nanosecond Nd:YAG and KrF excimer lasers were found to be less dependent on the laser fluence while they are affected appreciably by the fluence of femtosecond Ti:Sapphire laser. Addition of surfactants prevents the aggregation of Au nanoparticles after they were produced by nanosecond lasers while surfactants did not prevent the formation of Au clusters during femtosecond laser ablation. Nanosecond laser ablation in sodium dodecyl sulfate produced smaller particles than in 1-butanethiol, and 10^{-4} M concentration of $C_{12}H_{25}SO_4Na$ solution allows the formation of the smallest nanoparticles with narrowest particle size distributions. The lattice constants of Au nanoparticles produced by Ti:Sapphire laser are larger than those by Nd:YAG laser and the presence of surfactant $C_{12}H_{25}SO_4Na$ in the solution does not affect the lattice constants.

Acknowledgements

The authors are indebted to Mr. H. Reshef and Mr. Marco Zeman of the NRC-IMI London for their technical assistance.

References

- [1] J.J. Diao, J. Sun, J.B. Hutchison: Appl. Phys. Lett., 87, (2005) 103.
- [2] A.V. Kabashin, M. Meunier: J. Photoch & Photobio., 182, (2006) 330.
- [3] E. Jimenez, K. Abderrafi, J. Martinez-Pastor, R. Abarques, J. L. Valdes, R. Ibanez: Superlat. and Microstruc. doi:10.1016/J.spmi.2007.06.025.
- [4] R.M. Tilaki, A. Irajizad, S.M. Mahdavi: Appl. Phys. A, 84, (2006) 215.
- [5] J.P. Sylvestre, S. Poulin, A.V. Kabashin, E. Sacher, and M. Meunier: Appl. Phys. A, 80, (2005)753.
- [6] F. Mafunè, J. Kohno, Y. Takeda, and T. Kondow: J. Phys. Chem. B, 104, (2000) 9111.
- [7] J.P. Sylvestre, S. Poulin, A.V. Kabashin, E. Sacher, M. Meunier, and J.H.T. Luong: J. Phys. Chem. B, 108, (2004) 16864.
- [8] F. Mafunè, J.-Y. Kohno, Y. Takeda, T. Kondow: J. Phys. Chem. B, 106, (2002) 8555.
- [9] F. Mafunè, J.-Y. Kohno, Y. Takeda, T. Kondow, and H. Sawabe: J. Phys. Chem., 104, (2000) 8333.
- [10] F. Mafunè, J.-Y. Kohno, Y. Takeda, T. Kondow, and H. Sawabe: J. Phys. Chem. B., 105, (2001) 5144.
- [11] Y.-H. Chen and C.-S. Yeh: Colloids & Surfaces, 197, (2002) 133.
- [12] C. Schonberger, et al.: J. Phys. Chem., 99, (1995) 3259.

(Received: July 1, 2008, Accepted: October 28, 2008)